Temperature dependence of superconductor-correlated metal–superconductor Josephson junctions

J. K. Freericks[a] and B. K. Nikolić
Department of Physics, Georgetown University, Washington, D.C. 20057-0995

P. Miller
Department of Physics, Brandeis University, Waltham, Massachusetts 02454

(Received 5 August 2002; accepted 11 December 2002)

Josephson junctions, with the barrier composed of a correlated metal (or insulator) tuned to lie close to the metal–insulator transition, show promise to provide the fastest operating speeds for digital electronics based on rapid single-flux quantum logic. We provide theoretical calculations that indicate that these devices have a small enough temperature derivative of $I_c(T)$ within the junction operating range to allow them to be employed as elements in complex digital circuits. © *2003 American Institute of Physics.* [DOI: 10.1063/1.1543236]

Semiconductor-based digital electronics are rapidly reaching the upper limit of the circuit's operating speed. Silicon-based chips are not expected to be clocked much faster than 10 GHz, and circuits fabricated with faster semiconductors (such as InAs) are unlikely to be able to improve much more than one order of magnitude above the upper limit of silicon. Josephson-junction/based circuitry,[1] however, has a maximal operating speed that is significantly higher than that of semiconductor-based chips (flip-flop switches[2] have been demonstrated at over 700 GHz). The fundamental circuit element in superconductor-based electronics is the Josephson junction. Since the integral of a voltage pulse through a junction is equal to a flux quantum, the switching time is inversely proportional to the amplitude of the pulse [in rapid, single-flux quantum logic[3] (RSFQ)], which is determined by the product of the critical current at zero voltage I_c and the slope R_n of the $I-V$ characteristic at high voltage. Maximizing I_cR_n produces the fastest switching speeds in junctions.

In addition to a fast switching speed, RSFQ logic requires the $I-V$ characteristics to be nonhysteretic (with a McCumber parameter[4] $\beta \approx 1$). In conventional tunnel junctions, one adjusts the McCumber parameter by adding an external shunt resistor to the circuit. Finally, junctions need to have modest variation of $I_c(T)$ over the thermal operating range of the circuit, since variations in the switching speeds of the individual circuit elements (due to thermal variations) can cause the circuit to fail due to timing errors.

Recently, a class of Josephson junctions, the so-called superconductor-correlated metal–superconductor (SCmS) junctions, has been proposed as a means to optimize the switching speed of the junction.[5–9] A correlated metal (insulator) barrier is a barrier that lies close to the Mott–Hubbard-like metal–insulator transition, which may optimize the I_cR_n product. These junctions have been analyzed theoretically at low temperature, where it has been discovered that one can improve the switching speed by more than a factor of 4 [over the best externally shunted superconductor–insulator–superconductor (SIS) tunnel junctions] when the barrier lies just on the insulating side of the metal-insulator transition and is moderately thick.[7] Experiments have been carried out on junctions composed of NbTiN for the superconductor and of Ta-deficient Ta_xN for the barrier[8] (which can have its metallicity tuned by changing the number of Ta vacancies[10]). The results show a large I_cR_n when the barrier lies close to the metal-insulator transition, which occurs at $x=0.6$. Note that other types of Josephson junctions can have high I_cR_n products, like silicon barrier junctions,[11] where the semiconducting barrier is not a correlated metal; we focus here on SCmS junctions.

The two remaining questions that need to be addressed are the temperature dependence of these devices and the adjustment of β. Since β can be tuned by adding an external shunt resistor (if necessary), we do not address that issue in this contribution. Instead, we focus on the temperature dependence of the critical current and the characteristic voltage.

Our calculations are for wide junctions. We stack infinite two-dimensional planes, which describe either the superconductor or the barrier. A finite-sized sandwich is terminated to the left and to the right by semi-infinite superconducting leads (the superconducting gap and phase gradient differ from the bulk values only within the finite self-consistently modeled region which is about eight times the bulk superconducting coherence length). The superconductor is described by an attractive Hubbard model[12] in the Hartree–Fock approximation (equivalent to a BCS model,[13] except that the energy cutoff is determined by the bandwidth). The barrier is described by a Falicov–Kimball model (FK)[14] that contains two kinds of particles: conduction electrons and localized ions. The Coulomb correlations arise from the interaction between the electrons and ions when they occupy the same lattice site.

We solve the many-body, problem using an inhomohpgeneous generalization of dynamical mean field theory.[9,15] The original algorithm of Potthoff and Nolting[16] is generalized to include superconductivity via a Nambu–Gor'kov formalism.[17] Our calculations are fully self-consistent for the superconducting gap, the pair-field amplitude, and its phase.

[a]Electronic mail: freericks@physics.georgetown.edu

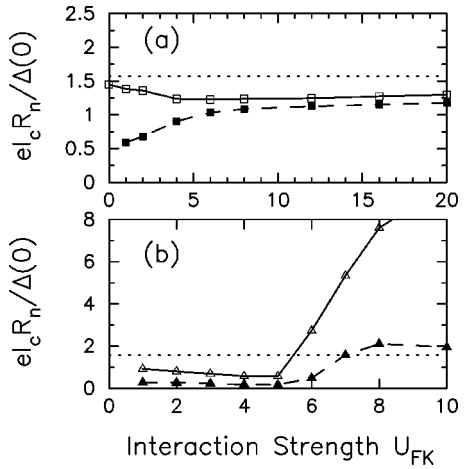

FIG. 1. Figure-of-merit I_cR_n [normalized by $\Delta(0)/e$] for (a) a thin ($N=1$) barrier and (b) a moderate ($N=5$) barrier at $T\approx T_c/11$ and $T\approx T_c/2$ as a function of the Coulomb interaction U_{FK}. The open symbols (and solid line) depict the low-temperature ($T\approx T_c/11$) results, and the solid symbols (and dashed line) depict the higher-temperature ($T\approx T_c/2$) results. The dotted line in both cases is the $T=0$ Ambegaokar–Baratoff (AB) prediction. Note how the single plane results are optimized in the metallic region for low T and in the insulating regime for high T, but the AB result is reduced by about 20%. In the five-plane case, the figure-of-merit is greatly enhanced on the insulating side of the metal–insulator transition. The large drop in I_cR_n at $T_c/2$ arises mainly from the reduction of $R_n(T)$ in the correlated metal (which probably has an exponential dependence on temperature).

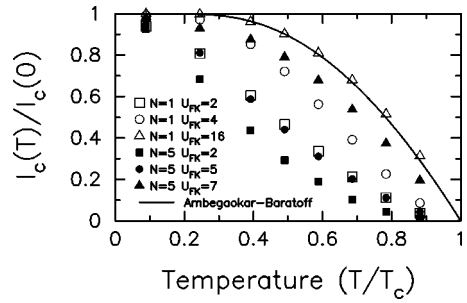

FIG. 2. Temperature dependence of the critical current for a variety of different Josephson junctions. The open symbols are for a single plane $N=1$ and the solid symbols are for a moderately thick $N=5$ junction. Each thickness has three different levels of correlation ranging from metallic $U_{\mathrm{FK}}=2$ to intermediate $U_{\mathrm{FK}}=4$ to insulating $U_{\mathrm{FK}}=16$ for the single-plane junction, and metallic $U_{\mathrm{FK}}=2$, to dirty metal $U_{\mathrm{FK}}=5$, to correlated insulator $U_{\mathrm{FK}}=7$ for the $N=5$ junction. In addition, we include the AB analytic result (solid line). Note how the thin insulator reproduces the AB result, and that the more metallic proximity-effect junctions have much steeper dI_c/dT.

We generate a current bias by introducing a phase gradient into the semi-infinite superconducting leads, and then self-consistently calculate the phase profile through the active region of the Josephson junction. The phase gradient is usually maximized at the central plane of the barrier, where the superconducting fluctuations are the weakest. The Josephson junction critical current is determined by the largest gradient that can be sustained and still maintain current conservation. We also calculate the normal state resistance. This is accomplished by employing a real-space Kubo formula for the current–current correlation function in the normal state. A separate determination of I_c and R_n allows us to calculate the figure-of-merit I_cR_n.

We choose the attractive Hubbard interaction to be $U_H=-2t$ for the superconducting planes (t is the nearest-neighbor hopping integral on a simple cubic lattice, which sets our energy scale). The bulk superconductor has a short coherence length ($\xi_s\approx 4a\approx 1.2$ nm) and is BCS-like: $T_c=0.112t$, $\Delta=0.198t$, and $2\Delta/k_BT=3.5$. The barrier is described by the FK model at half filling, which evolves from a dirty "Fermi liquid" metal (small U_{FK}) to a correlated insulator (large U_{FK}), with the transition occurring at $U_{\mathrm{FK}}\approx 4.9t$ in the bulk.

We first examine the figure-of-merit for a narrow junction of one plane in Fig. 1(a). We tune the metallicity of the plane from metallic to insulating by adjusting the FK interaction. In the bulk, the metal–insulator transition occurs at $U_{\mathrm{FK}}=4.9t$. We do not see insulating behavior for a single plane until the correlations are significantly stronger. We focus first on the low-temperature curve (at $T=0.01\approx T_c/11$). The region of the curve for $U_{\mathrm{FK}}>5$ shows the expected Ambegaokar–Baratoff prediction (AB)[18] that the figure-of-merit is independent of the value of the insulating gap (or equivalently of U_{FK}). It lies somewhat below their quantitative value (of $I_cR_n=\pi\Delta/2e$) because the short coherence length of the superconductor produces an "inverse proximity effect" where the superconductivity is suppressed as the superconductor–barrier interface is approached, reducing the effective gap value for the I_cR_n product.[9,15] We see a mild optimization of I_cR_n for the ballistic metal at $U_{\mathrm{FK}}=0$. (Note that these results differ slightly from those published earlier[7] due to an improved value for the normal-state resistance.) As we increase the temperature to $T=0.055\approx T_c/2$, the curve changes dramatically. We still see the constant curve for large correlations, but the characteristic voltage is dramatically reduced for small U_{FK}. This indicates that one needs to carefully optimize I_cR_n near the anticipated operating temperature of the junction.

We next examine the case of a moderately thick barrier of five planes in Fig. 1(b). At low temperature ($T\approx T_c/11$) and in the metallic phase, we see I_cR_n lies below the AB limit and decreases as the correlations increase, until the system hits a metal–insulator transition (at $U_{\mathrm{FK}}\approx 5.5t$), where the slope of the characteristic voltage changes sign to positive. I_cR_n continues to increase as correlations increase with a maximal value more than six times higher than the AB prediction. As we increase the temperature to $T\approx T_c/2$, we see the characteristic voltage is sharply decreased but still remains optimized for an insulator close to the metal–insulator transition ($U_{\mathrm{FK}}\approx 8t$). The total reduction increases as U_{FK} increases, with the majority of the reduction coming from the temperature dependence of $R_n(T)$. We feel the question of how much the *switching speed* will be reduced needs to be examined in a nonequilibrium formalism (that also includes junction capacitance effects), which we are currently carrying out, but SCmS junctions may need to be operated at lower temperatures than more conventional technologies.

In order to examine the thermal stability of the different enhanced values of I_cR_n, we perform calculations at a number of different temperatures for six different cases in Fig. 2. We compare these results to the AB prediction for the temperature dependence of $I_c(T)$ (solid curve), which is $I_cR_n=\Delta(T)\tanh[\Delta(T)/2T]$. We renormalize our results by an extrapolated value of $I_c(0)$, in order to plot all curves on one graph. As expected, we reproduce the AB result for the thin

insulator, but the other cases lie below. In general, we find that $I_c(T)$ decreases faster at low temperature (it appears to be linear) when the barrier is either more metallic or thicker. In the metallic cases, the rapid reduction of $I_c(T)$ will likely prevent such junctions from being used in circuits, due to the timing errors introduced by thermal variations. The moderately thick junction near a metal–insulator transition ($N=5$ and $U_{\mathrm{FK}}=7t$) has interesting behavior. While it decreases linearly (with a small slope) from $T=0$, it has approximately the same slope as the AB prediction for $0.4T_c<T<0.7T_c$. Hence, these junctions have a similar temperature dependence of the critical current as SIS junctions over the temperature range $0.4T_c<T<0.7T_c$ implying that a properly optimized SCmS junction can provide the best performance for RSFQ logic.

There are a few important points to note. First, the (low-T) derivative $dI_c(T)/dT$ is reduced for more insulating barriers, which explains why proximity-effect junctions are not commonly employed in digital circuits. Second, the properties of the Josephson junction depend strongly on the parameters of the barrier (thickness and U_{FK}) when we are close to optimization. This implies that it may be difficult to achieve good junction uniformity across a chip with SCmS junctions. The sensitivity to the parameters of the barrier is reduced at lower temperature though, indicating that lower temperature operation (say at about $0.2-0.3T_c$) may be preferable for SCmS junctions. Third, one still needs to determine whether the $I-V$ characteristics are hysteretic or nonhysteretic for use in RSFQ logic and how the speed varies with T. Such calculations require a nonequilibrium formalism and are beyond this work.

In conclusion, we have shown that SCmS junctions show great promise in being able to optimize Josephson junction switching speeds, but a number of theoretical, experimental, and engineering issues remain before successful implementation can be accomplished.

We acknowledge support from the Office of Naval Research under Grant No. N00014-99-1-0328. HPC time was provided by the Arctic Region Supercomputer Center. We also acknowledge useful discussions with T. Van Duzer, N. Newman, and J. Rowell.

[1] B. D. Josephson, Phys. Lett. **1**, 251 (1962).
[2] W. Chen, A. V. Rylyakov, V. Patel, J. E. Lukens, and K. K. Likharev, IEEE Trans. Appl. Supercond. **9**, 3212 (1999).
[3] O. A. Mukhanov, V. K. Semenov, and K. K. Likharev, IEEE Trans. Magn. **MAG-23**, 759 (1987); K. K. Likharev, in *Applications of Superconductivity*, edited by H. Weinstock (Kluwer, Dordrecht, 2000), Chap. 5.
[4] W. C. Stewart, Appl. Phys. Lett. **12**, 277 (1968); D. E. McCumber, J. Appl. Phys. **39**, 3113 (1968).
[5] A. S. Barrera and M. R. Beasley, IEEE Trans. Magn. **MAG-23**, 866 (1987).
[6] K. A. Delin and A. W. Kleinsasser, Supercond. Sci. Technol. **9**, 227 (1996); R. S. Decca, H. D. Drew, E. Osquiguil, B. Maiorov, and J. Guimpel, Phys. Rev. Lett. **85**, 3708 (2000).
[7] J. K. Freericks, B. K. Nikolić, and P. Miller, Phys. Rev. B **64**, 054511 (2001).
[8] A. B. Kaul, S. R. Whitely, T. Van Duzer, L. Yu, N. Newman, and J. M. Rowell, Appl. Phys. Lett. **78**, 99 (2001).
[9] J. K. Freericks, B. K. Nikolić, and P. Miller, Int. J. Mod. Phys. B **16**, 531 (2002).
[10] L. Yu, C. Stampfl, D. Marshall, T. Eshrig, V. Narayanan, J. M. Rowell, N. Newman, and A. J. Freeman, Phys. Rev. B **65**, 245110 (2002).
[11] C. L. Huang and T. Van Duzer, Appl. Phys. Lett. **25**, 753 (1974); IEEE Trans. Magn. **11**, 766 (1975).
[12] J. Hubbard, Proc. R. Soc. London, Ser. A **276**, 238 (1963).
[13] J. Bardeen, L. Cooper, and J. Schrieffer, Phys. Rev. **108**, 1175 (1957).
[14] L. M. Falicov and J. C. Kimball, Phys. Rev. Lett. **22**, 997 (1969).
[15] P. Miller and J. K. Freericks, J. Phys.: Condens. Matter **13**, 3187 (2001).
[16] M. Potthoff and W. Nolting, Phys. Rev. B **59**, 2549 (1999).
[17] Y. Nambu, Phys. Rev. **117**, 648 (1960).
[18] V. Ambegaokar and A. Baratoff, Phys. Rev. Lett. **10**, 486 (1963).